Program Digest, 2019 IEEE International Ultrasonics Symposium (IUS)
Glasgow, Scotland, October 6-9, 2019

Multi-wave dermis characterization using attenuation coefficient and shear wave speed estimates *in vivo*

Ana Cecilia Saavedra*, Benjamin Castaneda*, and Roberto J. Lavarello*
*Laboratorio de Imágenes Médicas, Departamento de Ingeniería, Pontificia Universidad Católica del Perú,
San Miguel, Lima, Perú.

***Abstract*—Skin characterization is of importance for disease diagnosis and treatment follow-up. In particular, estimation of the biomechanical properties is useful for wound healing monitoring. This study proposes and validates for the first time the use of multi-wave quantitative ultrasound (MWQUS) as a skin characterization tool via the estimation of attenuation coefficient slope (ACS) and shear wave speed (SWS) *in vivo* based on the regularized spectral-log difference technique (RSLD) and crawling wave sonoelastography (CrW). Nine volunteers without skin injuries (age range of 19-30 years) were scanned in the middle of the dorsal side of the forearm. The median of the ACS and SWS were 1.93 dB$\cdot$cm$^{-1}\cdot$MHz^{-1} and 3.24 m/s, respectively, which are in good agreement with previous reports in the literature. Results showed a decreasing trend of the SWS with increasing ACS with a statistically significant (p = 0.01) Pearson correlation coefficient of -0.79. The importance of the results presented here lies in that the observed variability in the estimates appears to stem from biological variability jointly explained by both ACS and SWS parameters. These results suggest that both methodologies (RSLD and CrW) can be applied together for a more complete, comprehensive multi-wave QUS characterization of the skin and provide estimates that are sensitive to changes in dermal composition.**

***Index Terms*—attenuation coefficient, elastography, crawling wave sonoelastography, surface acoustics waves, shear waves, high-frequency ultrasound, skin.**

I. Introduction

Skin disorders affect humans in a great variety of symptoms and severity. High-frequency ultrasound (HF-US) is a non-invasive imaging tool, which refers to the use of ultrasonic waves with frequencies higher than 15 MHz. This imaging modality has been used for research skin aging, application of cosmetic fillers, skin cancer description, wound healing, among others [1].

Skin characterization is of importance for disease diagnosis and treatment follow-up. Biomechanical properties of the skin can be estimated using quantitative ultrasound techniques (QUS). The attenuation coefficient slope (ACS) measures the rate of acoustic energy loss when the US signal propagates through a medium. Previous studies have reported the ACS of the human dermis *in vivo*. Guittet *et al.* [2] reported values ranging from 0.7 to 3.6 dB $\cdot$ cm^{-1} $\cdot$ MHz^{-1} for the forearm dermis. Raju *et al.* [3] estimated dermal ACS in the forearm and fingertip, obtaining a higher value in the latter. Recently, the regularized spectral-log difference (RSLD) method was used for estimating the ACS in the forearm and thigh dermis, reporting a significant difference between both locations [4].

The shear wave speed (SWS) is estimated by monitoring shear wave propagation and is related to the stiffness of the underlying tissues. This parameter is estimated using elastographic methods. Supersonic shear imaging (SSI) and inverse analysis were used to calculate the skin elastic properties [5]. Furthermore, a laser vibrometer technique was used to characterize the skin in several anatomical sites [6]. Also, shear wave elastography (SWE) [7] and shear wave elasticity imaging (SWEI) [8] have been used to compare skin stiffness in healthy and sclerotic regions. Recently, crawling wave sonoelastography was used with an HF-US system for the estimation of surface acoustic waves [9], and its application for estimating the SWS of the thigh dermis [10].

This study proposes and validates for the first time, the use of multi-wave quantitative ultrasound (MWQUS) as a skin characterization tool via the estimation of ACS and SWS *in vivo*.

II. Methodology

A. Acquisition protocol

Nine volunteers (seven males and two females) without skin injuries and in the age range of 19-30 years (24.3$\pm$3.8) participated in this study. The study was approved by the institutional review board of the Pontificia Universidad Catolica del Peru and informed consents were obtained from all participants. The dorsal side of the forearm was considered for the assessment.

The acquisition was performed using a Vevo 2100 system (Fujifilm Visualsonics Inc., Toronto, ON, Canada) equipped with an MS250 linear transducer. The anatomical site was marked with a water-resistant marker. The scanner was set in B-mode, and a preliminary free-hand examination of the skin was operated. The setup for generating the external vibration included two mini-shakers (Type 4810; Bruel & Kjær, Nærum, Denmark), a signal wave generator (AFG3252; Tektronix, Beaverton, OR, USA) and two amplifiers (Type 2718; Bruel & Kjær). A comfortable position was found for the scanning. The probe was located in the middle of the forearm in a parallel direction to the Langer's line with a layer of US-gel. The vibration sources were placed at the sides and were controlled by the amplifiers and the wave generator. When the system was set in the power Doppler mode, the amplitudes of both mini-shakers were calibrated individually. A vibration frequency of 200 Hz with a 0.4 Hz offset to form the motion pattern was configured. Several grayscale images from the Doppler mode and B-mode were acquired. Finally, data from an agar-based reference phantom with embedded glass beads of 3.2 μm diameter was obtained with the same scanner settings used for volunteer scanning.

B. ACS estimation: Regularized spectral-log difference technique

The spectral-log difference technique calculates the attenuation coefficient by dividing the region of interest (ROI) into proximal and distal sub-regions. The power spectrum of any of the windows can be described as [11]

$$S_s(f,z) = P(f)D(f,z)\eta_s(f,z)A_s(f,z_0)e^{-4\alpha_s(f)(z-z_0)} \ , \tag{1}$$

where z corresponds to the depth of the center of either the proximal z_p or distal z_d sub-regions, and z_0 is the depth of the top of the block. The $P(f)$ term corresponds to the scanner transfer function, $D_s(f)$ denotes the diffraction effects, $A_s(f,z_0)$ represents the total attenuation of the echoes between the transducer and the top of the block, η_s is the backscatter and $\alpha_s(f)$ is the attenuation of the sub-region.

Diffraction effects are compensated by using a calibrated reference phantom. When replacing z for the distal and proximal case in (2), the log-ratio $Y(f)$ of the total ROI satisfies

$$Y(f) = 4(z_p - z_d)\alpha_s(f) + \ln\frac{[S_s(f,z_d)/S_{ref}(f,z_d)]}{[S_s(f,z_p)/S_{ref}(f,z_p)]} \ , \tag{2}$$

where $S_s(f,z)$ and $S_{ref}(f,z)$ denotes the power spectrum of the sample and reference phantom, respectively. Assuming a linear dependence of the attenuation coefficient with frequency, $Y(f)$ can be rewritten as

$$Y(f) = 4(z_p - z_d)\beta \cdot f + c \ . \tag{3}$$

The RSLD technique calculates the attenuation coefficient slope, extending the precision vs. spatial resolution trade-off of the SLD technique [12]. The ACS is estimated as

$$\min_{B,C}\left\{\frac{1}{2}\|Y - F\begin{bmatrix}B\\C\end{bmatrix}\|_2^2 + \mu\cdot(TV(B)+TV(C))\right\} \ , \tag{4}$$

where B and C vectors refer to the ACS and the ratio of the backscatter coefficients between the proximal and distal sub-windows, respectively. The matrix F relates the measurements Y to the unknown vectors B and C. The term $\|\cdot\|_2^2$ is the data fidelity term, the scalar μ is the regularization parameter and $TV(\cdot)$ is the total variation (TV) operator.

C. SWS estimation: Crawling wave sonoelastography

Crawling wave (CrW) sonoelastography was used for the estimation of SWS via generation and analysis of surface acoustic waves. The generation of a dynamic interference pattern allows estimating wave propagation by propagating to waves opposed to each other [13]. The square amplitude of the wave motion-induced parallel to the x-axis through time can be mathematically established as

$$|u(x,t)|^2 = 2e^{(-\gamma D)}\left[A + \cos[(2k+\Delta k)x + \Delta\omega t - \varphi_0]\right] \ , \tag{5}$$

where A and γ refer to the DC value and the shear attenuation coefficient, respectively. The term D corresponds to the separation distance of both vibration sources. The variable $\Delta\omega$ describes the frequency offset, whereas k is the wavenumber. The last term φ_0 denotes a constant (i.e., $\frac{\Delta k}{2}D + \Delta\varphi$), where $\Delta\varphi = \phi_r - \varphi_l$. In (5), $2k$ indicates the spatial frequency of the pattern, which corresponds to half the acoustic wavelength. Hence, the wave speed can be estimated as the product of the vibration source frequency and the wavelength of the crawling wave interference pattern [13].

The phase-based estimator computes the velocity of propagation in the slow-time, as explained in [14]. Additionally, extracting the spatial phase $\tilde{\phi}$ of (5) leads to

$$\tilde{\phi} = 2kx + (\frac{\Delta k}{2})D - \Delta\varphi \ , \tag{6}$$

Given that surface acoustics waves are the ones being propagated, a compensation factor must be applied to reach the shear wave speed value [6], and for a vibration frequency f_s, the SWS can be estimated as

$$c = 1.05\frac{4\pi f_s}{\tilde{\phi}'(x)} \ , \tag{7}$$

where $\tilde{\phi}'(x)$ corresponds to the spatial derivative of $\tilde{\phi}(x)$.

D. Data processing

The in-phase and quadrature (IQ) components, as well as Doppler motion, were exported from the Vevo 2100 and imported to MATLAB® (Mathworks, Natick, Massachusetts, USA). IQ signals were converted to radio frequency signals for estimating the ACS of the volunteers. The RSLD method was used in bandwidth from 8 to 27 MHz. The same axial and lateral position of the selected ROI in the sample data was selected in the reference phantom data. The two ROIs were split into several overlapped sub-ROIs (80%) through all the domain. Then, after the sub-division of each sub-ROI, (4) was used for obtaining the ACS map.

The Kasai algorithm was implemented for processing the CrW motion from the Doppler data. The mean amplitude was subtracted and a median filter was applied. The remaining CrW video was employed for the estimation of the spatial derivative, which was subsequently replaced in (7).

III. Results

A. Attenuation coefficient slope

The wavelength λ at the center frequency of the analysis bandwidth was 0.09 mm. The window size was set to $8\lambda \times 8\lambda$. The estimated ACS for a volunteer was calculated as the median of estimates on at least two data frames. On the whole, the ACS in the forearm dermis was 1.93 ± 0.38 dB $\cdot$ cm^{-1} $\cdot$ MHz^{-1}. Figure 1 (b) shows the B-mode image and the ACS map from one representative volunteer in the forearm.

B. Shear wave speed

The median and standard deviation estimates at the vibration frequency of 200 Hz were 3.24 $\pm$0.56 m/s for the target group. An illustration of the SWS map obtained for the forearm dermis of one volunteer is shown in Figure 1 (c).

C. Statistical analysis

A linear regression approach was applied to the estimates of ACS and SWS to model the relationship between both parameters per volunteer. Figure 1 (a) shows the plot of the SWS vs. the ACS per volunteer. A decreasing trend of the SWS is observed when the ACS increases (i.e., SWS= -1.6 dB$^{-1}\cdot$ cm $\cdot$ MHz $\cdot$ m $\cdot$ s$^{-1}\times$ ACS $+6.2$ m $\cdot$ s^{-1}). In addition, the linear regression revealed a statistically significant ($p = 0.01$) Pearson correlation coefficient of -0.79.

IV. Discussion

Multi-wave quantitative ultrasound was performed in the forearm dermis *in vivo*. The estimated ACS and SWS values agree with those reported by previous studies in the same anatomical site, as shown in Table 1.

TABLE I
Comparison between the ACS and SWS of the forearm dermis reported in the literature and this study.

Parameter	Method	Value	Age	Ref.
ACS (dB/cm/MHz)	RSLD	1.93	19-30	This study
	Centroid algorithm	2.63	15-30	[2]
	Slope vs. depth	2.1	19-36	[3]
	RSLD	2.07	19-27	[4]
SWS (m/s)	CrW	3.24	19-30	This study
	Laser vibrometer	3.79	27-50	[6]
	USWE[a]	3.45	22-73	[15]

[a]Ultrasound surface wave elastography.

Regarding ACS results, there is a difference of 26% concerning the values reported in [2]. This fact may be explained by the differences in the age of the volunteers considered for the study. As expected, younger participants have higher ACS estimates. SWS values show good agreement with the other two studies. The maximum discrepancy is approximately 15% with [6], which may also be attributed to the different range of ages. Several works [16]–[18] showed an increasing trend SWS as a function of age.

In this study, a negative correlation between ACS and SWS was observed. This result appears to be due to biological variations in skin composition among volunteers and is consistent with reports in the literature on the effects of aging in QUS estimates from dermal tissues. Previous studies have reported a decrease of the ACS and an increase of the SWS with increasing age. Guittet *et al.* [2] reported a negative trend of ACS with respect to the age (slope= -0.024 dB $\cdot$ cm$^{-1}\cdot$ MHz$^{-1}\cdot$ yrs.$^{-1}$) in human skin *in vivo*. Similarly, Bhagat and Kerrick reported that the dermal ACS in 2-month old mice was nearly twice as large as the one in 27-month old mice in the frequency range from 5 to 10 MHz [19]. Concerning the SWS, Davis *et al.* [16] reported a positive relationship between velocity and age (slope $= 0.25$ m $\cdot$ s$^{-1}\cdot$ yrs.$^{-1}$). Similarly, an increasing trend of the Young's Modulus as a function of age has been estimated for men (slope ≈ 1.95 KPa $\cdot$ yrs.$^{-1}$) and women (slope ≈ 0.27 KPa $\cdot$ yrs.$^{-1}$) [17]. Grahame and Holt [18] also reported a positive tendency when age rises (slope ≈ 0.13 dyn $\cdot$ cm$^{-2}\cdot$ yrs.$^{-1}$). Given that several factors affect QUS parameters in the skin (e.g., collagen and elastin content and arrangement and hydration, among others), further work is required to fully understand the mechanism behind the observed correlation between ACS and SWS.

To our knowledge, no previous studies have related ACS and SWS for a particular age stage. It is worth noting that the two biomarkers were estimated from the same scanner, although they are extracted from different waves (i.e., longitudinal and shear). This multi-wave characterization may lead to a more comprehensive assessment of the skin and shows the feasibility of a multi-parametric estimation using HF-US.

V. Conclusion

This study presents the first attempt of a multi-wave QUS characterization of the skin. Results from this work suggest that both methodologies (RSLD and CrW) can be applied together for a more complete, comprehensive QUS characterization of the skin and provide estimates that are sensitive to changes in dermal composition.

References

[1] X. Wortsman, *Atlas of Dermatologic Ultrasound*. Springer, 2018.
[2] C. Guittet, F. Ossant, L. Vaillant, and M. Berson, “In vivo high-frequency ultrasonic characterization of human dermis,” *IEEE Transactions on Biomedical Engineering*, vol. 46, no. 6, pp. 740–746, 1999.
[3] B. I. Raju and M. A. Srinivasan, “High-frequency ultrasonic attenuation and backscatter coefficients of in vivo normal human dermis and subcutaneous fat,” *Ultrasound in Medicine and Biology*, vol. 27, no. 11, pp. 1543–1556, 2001.
[4] A. C. Saavedra, A. Coila, J. Arroyo, B. Castaneda, and R. J. Lavarello, “In vivo attenuation coefficient estimation in the healthy forearm and thigh human dermis,” in *2018 IEEE International Ultrasonics Symposium (IUS)*. IEEE, 2018, pp. 1–4.
[5] C.-C. Luo, L.-X. Qian, G.-Y. Li, Y. Jiang, S. Liang, and Y. Cao, “Determining the in vivo elastic properties of dermis layer of human skin using the supersonic shear imaging technique and inverse analysis,” *Medical physics*, vol. 42, no. 7, pp. 4106–4115, 2015.
[6] X. Zhang, T. G. Osborn, M. R. Pittelkow, B. Qiang, R. R. Kinnick, and J. F. Greenleaf, “Quantitative assessment of scleroderma by surface wave technique,” *Medical engineering & physics*, vol. 33, no. 1, pp. 31–37, 2011.
[7] X. Xiang, F. Yan, Y. Yang, Y. Tang, L. Wang, J. Zeng, and L. Qiu, “Quantitative assessment of healthy skin elasticity: reliability and feasibility of shear wave elastography,” *Ultrasound in medicine & biology*, vol. 43, no. 2, pp. 445–452, 2017.
[8] S. Y. Lee, A. R. Cardones, J. Doherty, K. Nightingale, and M. Palmeri, “Preliminary results on the feasibility of using arfi/swei to assess cutaneous sclerotic diseases,” *Ultrasound in medicine & biology*, vol. 41, no. 11, pp. 2806–2819, 2015.
[9] A. C. Saavedra, F. Zvietcovich, R. J. Lavarello, and B. Castaneda, “Measurement of surface acoustic waves in high-frequency ultrasound: Preliminary results,” in *Engineering in Medicine and Biology Society (EMBC), 2017 39th Annual International Conference of the IEEE*. IEEE, 2017, pp. 3000–3003.
[10] A. C. Saavedra, J. Arroyo, F. Zvietcovich, R. J. Lavarello, and B. Castaneda, “In vivo estimation of the Young's modulus in normal human dermis,” in *Engineering in Medicine and Biology Society (EMBC), 2018 40th Annual International Conference of the IEEE*. IEEE, 2018, *in press*.

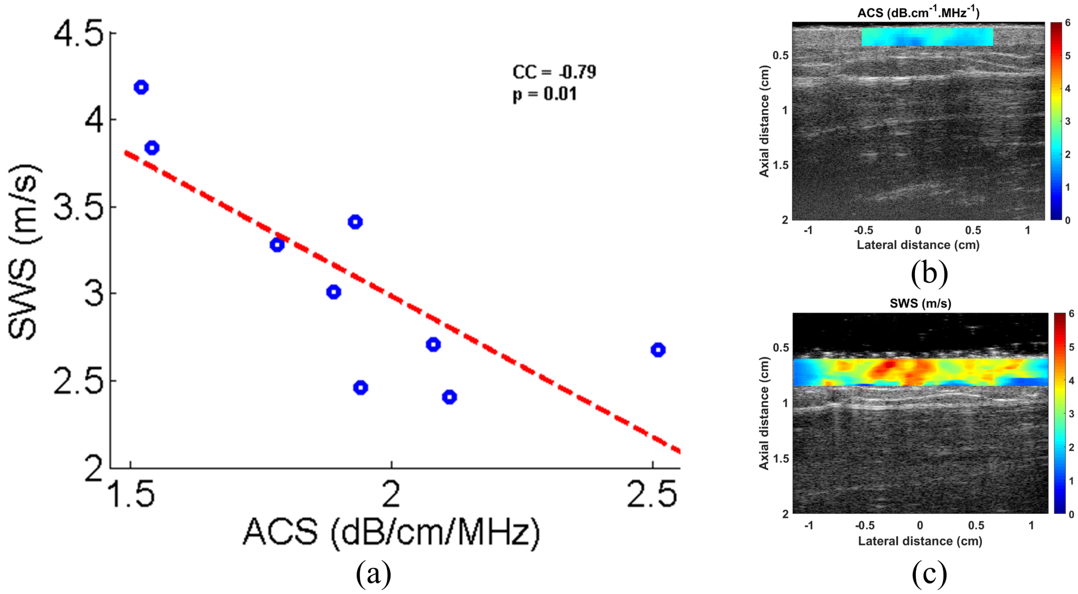

Fig. 1. (a) SWS vs. ACS and the linear regression (red dashed line). (b) B-mode image and ACS maps of the healthy forearm. (c) B-mode image and SWS maps of the healthy forearm.

[11] Y. Labyed and T. A. Bigelow, "A theoretical comparison of attenuation measurement techniques from backscattered ultrasound echoes," *The Journal of the Acoustical Society of America*, vol. 129, no. 4, pp. 2316–2324, 2011.
[12] A. L. Coila and R. Lavarello, "Regularized spectral log difference technique for ultrasonic attenuation imaging," *IEEE Transactions on Ultrasonics, Ferroelectrics, and Frequency Control*, vol. 65, no. 3, pp. 378–389, 2018.
[13] Z. Wu, L. S. Taylor, D. J. Rubens, and K. J. Parker, "Sonoelastographic imaging of interference patterns for estimation of the shear velocity of homogeneous biomaterials," *Physics in Medicine & Biology*, vol. 49, no. 6, p. 911, 2004.
[14] Z. Hah, C. Hazard, B. Mills, C. Barry, D. Rubens, and K. Parker, "Integration of crawling waves in an ultrasound imaging system. part 2: signal processing and applications," *Ultrasound in Medicine and Biology*, vol. 38, no. 2, pp. 312–323, 2012.
[15] X. Zhang, B. Zhou, S. Kalra, B. Bartholmai, J. Greenleaf, and T. Osborn, "An ultrasound surface wave technique for assessing skin and lung diseases," *Ultrasound in medicine & biology*, vol. 44, no. 2, pp. 321–331, 2018.
[16] B. R. Davis, E. Bahniuk, J. K. Young, C. M. Barnard, and J. M. Mansour, "Age-dependent changes in the shear wave propagation through human skin," *Experimental gerontology*, vol. 24, no. 3, pp. 201–210, 1989.
[17] S. Diridollou, V. Vabre, M. Berson, L. Vaillant, D. Black, J. Lagarde, J. Grégoire, Y. Gall, and F. Patat, "Skin ageing: changes of physical properties of human skin in vivo," *International journal of cosmetic science*, vol. 23, no. 6, pp. 353–362, 2001.
[18] R. Grahame and P. Holt, "The influence of ageing on the in vivo elasticity of human skin." *Gerontologia*, vol. 15, no. 2, p. 121, 1969.
[19] P. Bhagat, W. Kerrick, and R. Ware, "Ultrasonic characterization of aging in skin tissue," *Ultrasound in medicine & biology*, vol. 6, no. 4, pp. 369–375, 1980.